Steady state tyre behaviour with emphasis on local contact phenomena

Joop P. Pauwelussen
HAN University

P.O. Box 2217
6802 CE Arnhem, The Netherlands
Phone: +31 26 36582976
Fax.: +31 26 365 8126
joop.pauwelussen@ft.han.nl

ABSTRACT

Research on tyre handling behaviour was originally aimed at deriving the tyre performance characteristics. Motivation has now moved to more environmentally related tyre properties such as reduction of tyre wear, noise emission, rolling resistance, improved tyre braking properties in relationship with vehicle and suspension behaviour and road conditions. One way to approach these problems is to use a detailed tyre model to obtain a realistic quantitative description of the tyre-road interface using a highly discretised patch model in combination with some physical belt model. However, since we do not even understand local contact phenomena based on simple analytical models, such quantitative analysis results will be very difficult to interpret.
This paper deals with such an analytical tyremodel accounting for both the belt (modelled as a stretched string) and the treads (modelled as brush elements). Bare stretched string tyremodels (i.e. without treads) are quite commonly used as stand-alone model in case of pure slip under steady and transient conditions. Combined braking and cornering has been studied only for the bare tyre model. Sofar, the extension with treadelements is limited to lateral slip under restrictive conditions.
In this paper, these omissions are corrected and the **combined brush-string model** is treated for arbitrary combination of combined slip and tyre properties such as carcass stiffness, tread stiffness and relaxation length. The solution of the steady state contact problem is derived using the socalled **singular integral approach** to describe the flexibility-properties of the tyre with the local tyre deflections expressed in terms of integrals of shear stress over the contact area using certain kernel functions. This approach can be generalised to any tyre model including FEM, making it a potentially very powerful tool to extend the qualitative results of this paper to a more quantitative analysis in a straightforward manner. The steady state solution is discussed for various combinations of tyre properties.

Keywords / tyre property, tyre slip, tyre model, simulation technology

1. INTRODUCTION

The earliest motivation for describing the steady state behaviour of a tyre was to derive the relationship between contact shearforces and tyre slip. This has resulted in pragmatic tyre models such as Pacejka's model and physical tyre models to interpret these relationships qualitatively in terms of tyre stiffness parameters, road friction, etc. Many of these physical models usually include some kind of compliance-model for the belt-response, possibly in combination with a tread model described as little flexible beams (brushes) connected radially to the belt.

Sofar, the local contact phenomena between tyre and road were not getting much attention. The need to improve tyredesign with respect to local wear, noise emission, rolling resistance, etc., being all global tyre properties depending very much on the local contact phenomena, has changed that. See figure 1 for a typical shear stress pattern for a rolling tyre.

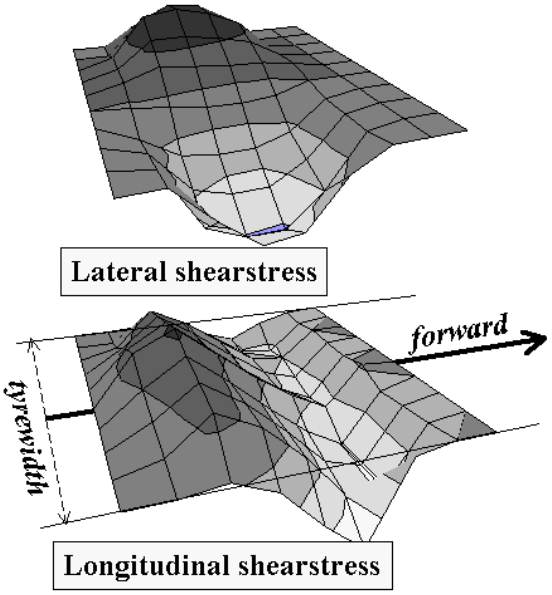

Fig 1.: Typical shearstresses for a rolling tyre

One might decide to use Finite Elements to derive a realistic quantitative description of these phenomena. However, there are hardly any facilities around the world that are able to derive reliable measurement results on local shearforces which makes the reliability of these models doubtful.

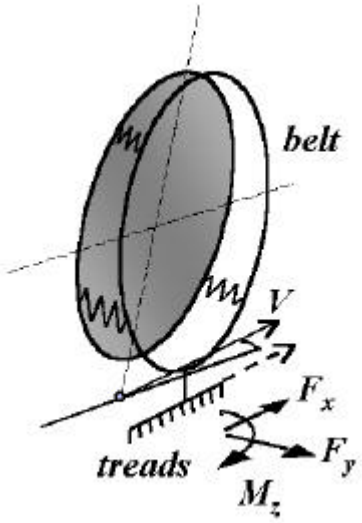

Fig. 2.: Layout of the brush-string model.

This paper deals with the **brush-string model**, combining a stretched string description of the belt with a brush-type description of the treads, see figure 2. The bare stretched string model (i.e. withour treads) has been applied extensively by many researchers in case of steady state pure slip (von Schlippe, Segel, Pacejka, Besselink). Higuchi extended it to combined slip. Pacejka combined it with tread elements (brushes) for specific combinations of tread- and carcass-stiffness.

The brush-string model can be regarded as the link between the two extreme cases of the stand-alone brush model (with the carcass-stiffness exceeding the tread stiffness by far) and the bare string model (i.e. with extremely high tread stiffness). The status for the brush-string model as well as for its extreme cases of bare string and brush model are indicated in table 1.

Tyre model	*Pure slip*	*Combined slip*
Brushes only	Well established	Well established
Brush-string	Restricted to one sliding region at the rear (Pacejka)	not available
Bare string	(Pacejka)	(Higuchi)

Table 1.: Status of various theoretical tyre models

Both the brush-model and the bare string model have been well examined, in contrast to the more general brush-string model. In the next sections, this model will be formulated and solved using the so-called **singular integral approach** which is quite common in the analysis of partial differential equations. This means that the local tyre deflections are described as a superposition of deflections from local unit shear stresses using kernel functions usually referred to as Green functions. The advantage of this approach is that these kernel functions are not restricted to analytical belt models but can be derived from any tyre model including FEM. They reduce the analysis of the flexibility of a complex 3D tyre-structure to the solution of a set of integral equations in terms of contact properties, which makes this approach a potentially very powerful tool to analyse local contact phenomena.

2. THE COMBINED BRUSH-STRING MODEL

The model is outlined in figure 3. Points of the tyre may be either fixed to the road (**adhesion region**, implying a zero sliding speed) or may be sliding (**sliding region** with the shear stress proportional to the normal stress, according to Coulomb's law). Two deflections are distinguished in longitudinal and lateral direction, u and v, respectively, made up out of the tread deflection (subscript t) and the belt deflection (subscript b):

$$u = u_t + u_b \quad , \quad v = v_t + v_b \tag{1}$$

These deflections are assumed to be averaged over the width of the contact area, i.e. depending on the longitudinal co-ordinate x only.

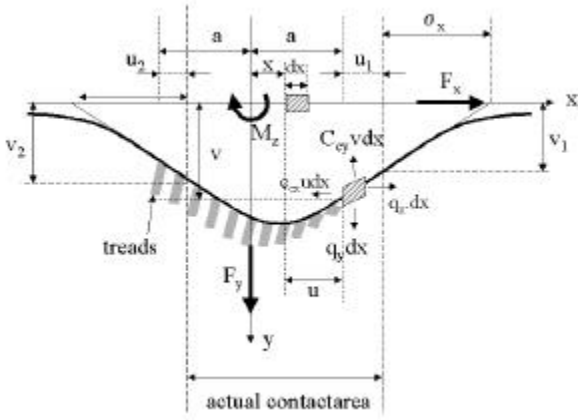

Fig. 3.: The brush-string model

As treated by Pacejka in [2], the belt-deflections satisfy the following equations:

$$s_x^2 \cdot \frac{d^2 u_b}{dx^2} - u_b = -\frac{q_x}{c_{cx}} \quad ; -a < x < a \tag{2a}$$

$$s_y^2 \cdot \frac{d^2 v_b}{dx^2} - v_b = -\frac{q_y}{c_{cy}} \quad ; -a < x < a \tag{2b}$$

with half contactlength a, longitudinal and lateral carcass stiffnesses c_{cx} and c_{cy}, relaxation lengths σ_x, σ_y with respect to longitudinal and lateral slip, and shear forces per unit length q_x and q_y. The tread deflections are proportional to these shearforces with tread stiffnesses denoted by c_{px} and c_{py}:

$$q_x = c_{px}.u_t \ , \ q_y = c_{py}.v_t \ ; \text{-a < x < a} \qquad (3)$$

A bounded solution outside the contactarea implies the mixed boundary conditions:

$$\frac{du_b(\pm a)}{dx} = \mp \frac{u_b(\pm a)}{s_x} \ , \ \frac{dv_b(\pm a)}{dx} = \mp \frac{v_b(\pm a)}{s_y} \qquad (4)$$

We assume, for simplicity, a quadratic normal tyre force per unit length:

$$q_z = Q.(1 - \left(\frac{x}{a}\right)^2 \qquad (5)$$

In the sliding region, Coulomb law implies:

$$q_{shear} \equiv \sqrt{q_x^2 + q_y^2} = m.q_z \qquad (6)$$

Neglecting the tyre yaw velocity, assuming small slip angles and restricting to steady state behaviour, the sliding speed components V_{gx} and V_{gy} within the contactarea can be expressed as (see [2]):

$$V_{gx} = -V(1+k).\left(z_x + \frac{du}{dx}\right) \qquad (7a)$$

$$V_{gy} = -V(1+k).\left(z_y + \frac{dv}{dx}\right) \qquad (7b)$$

for tyre forward speed V, practical brakeslip κ, theoretical slipvalues ζ_x, ζ_y. Hence, in the adhesion region with vanishing sliding speeds V_{gx} and V_{gy}, the delfections vary linearly over the contactarea:

$$\frac{du}{dx} = -z_x, \frac{dv}{dx} = -z_y \qquad (8)$$

The brush-string model allows two sliding regions, (-a, a_2) and (a_1, a) at the trailing and leading edges, similar to the bare belt model (see [1]), but in contrast to the brush model which only allows one sliding area at the trailing edge. In case of two sliding regions, shearforces are assumed ot be continous over the entire contactarea, and differentiable at x = a_1 (and consequently a continuous sliding speed at the first leading boundary of the adhesion area). Consequently, a continuous sliding speed cannot be guaranteed at the breakaway point a_2 between sliding and adhesion region. It should be noted that, for the brush-model, the sliding speed isn't continuous at this point either.

3. THE SINGULAR INTEGRAL FORMULATION

The differential equations (2a) and (2b) in combination with boundary conditions (4) are equivalent to the following singular integral equations:

$$u_b(x) = \int_{-a}^{a} G_{xx}(x;x).q_x(x)dx \qquad (9a)$$

$$v_b(x) = \int_{-a}^{a} G_{yy}(x;x).q_y(x)dx \qquad (9b)$$

for known kernel functions G_{xx}, G_{yy} (usually denoted as Green functions), solving the singular differential equations on (-a, a):

$$s_x^2.\frac{\partial^2}{\partial x^2}G_{xx} - G_{xx} = -\frac{d(x-x)}{c_{cx}} \qquad (10a)$$

$$s_y^2.\frac{\partial^2}{\partial x^2}G_{yy} - G_{yy} = -\frac{d(x-x)}{c_{cy}} \qquad (10b)$$

for Dirac Delta function $\delta(x)$ satisfying:

$$d(x) = 0 \qquad ; \ x \neq 0$$

$$\int_{-e}^{e} d(x)dx = 1 \quad ; \text{for all } e > 0$$

We want to apply conditions (8). For that reason, (9) is differentiated with respect to x, yielding together with (1) and (3):

$$\frac{du}{dx} - \frac{1}{c_{px}}.\frac{dq_x}{dx} = \int_{-a}^{a} H_{xx}(x;x).q_x(x)dx \qquad (11)$$

and likewise in y-direction, with H(x, ξ) being the deriviative of G(x, ξ) in the first variable.
Within the adhesion area, (11) results in the equation

$$z_x + \frac{1}{c_{px}}.\frac{dq_x}{dx} + \int_{-a}^{a} H_{xx}(x;x).q_x(x)dx = 0 \qquad (12)$$

for ***any point*** in the adhesion area!
A physical interpretation of the Green function can be given as follows, where we consider the general case with deflections u_b and v_b and shearforces q_x and q_y depending on x and y, cf. fig.1. Assuming the case of a local unit shearforce acting at a single point (ξ,η), one arrives at a distribution of belt deflection (u_b, v_b) at arbitrary points (x, y) of the contact area, and with these deflections corresponding to the Green functions (indicated in fig. 4).

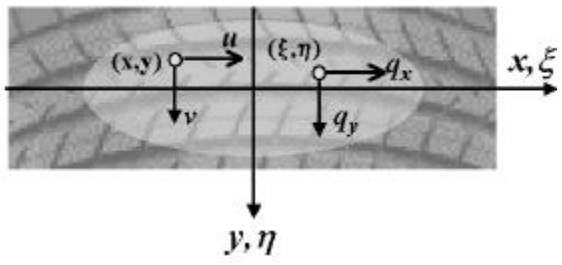

Fig. 4.: Interpretation of the Green function

Summing up local isolated shearforces to a general shear force distribution results in a superposition of the corresponding deflection distributions over the contact area. This superposition is expressed by equations (10). These observations also hold for any tyre model such as for example FEM, allowing the extension of this Singular Integral approach, see [4] for a detailed discussion.
The solution $G_{xx}(x;\xi)$ of (10a) satisfying (4) is given by:

$$G_{xx}(x;x) = \frac{1}{2.c_{cx}.s_x}.e^{\frac{x-x}{s_x}} \quad ; x < \xi$$

$$G_{xx}(x;x) = \frac{1}{2.c_{cx}.s_x}.e^{\frac{x-x}{s_x}} \quad ; x > \xi$$

and likewise for $G_{yy}(x;\xi)$.

4. THE STEADY STATE CONTACT PROBLEM

The total sliding speed vanishes in the adhesion part of the contact area, which is identical to stating that (see equation (7)):

$$u(x) = -z_x(x-a_1)+u_1 \quad ; a_2 < x < a_1 \le a \qquad (13a)$$

$$v(x) = -z_y(x-a_1)+v_1 \quad ; a_2 < x < a_1 \le a \qquad (13b)$$

for some unknown $u_1 = u(a_1)$ and $v_1 = v(a_1)$. Combination of (11) with (1) and (3) leads to:

$$u_b(x) = -z_x(x-a_1)+u_1-\frac{q_x(x)}{c_{px}} \quad ; a_2 < x < a_1 \le a$$

$$v_b(x) = -z_y(x-a_1)+v_1-\frac{q_y(x)}{c_{py}} \quad ; a_2 < x < a_1 \le a$$

Substitution of these expressions in (2) leads to second order equations in the shear forces on the adhesion part of the contact area in terms of unknowns u_1, v_1, a_1, a_2 and some integration constants. On the sliding area, the shear forces follow from Coulomb law cf. (6) with the orientation of the shear force vector still to be determined. All of these unknowns can be determined from (12) for given brakeslip- and lateral slipvalues (κ, α), or equivalently, given theoretical slipvalues (ζ_x, ζ_y). For that reason, the expressions for the shear forces are substituted in (12) after which (12) is solved for a sufficient number of x-values in the adhesion region. We note here that (12) is nonlinear in the orientations of the shear force vector as well as in the 'break away'-points a_1 and a_2. Newton-iteration appears to work very well.

5. MODEL OUTPUT

We have solved the above model for the following set of parameters, in accordance with the work of Higuchi, see table 2.

a	0.05 [m]
c_{cx}	6.81×10^6 [N/m^2]
c_{cy}	6.17×10^6 [N/m^2]
F_z	3000 [N]
μ	1 [-]
σ_x	0.01 [m]
σ_y	0.02 [m]

Table 2.: Parameters used in the calculations

Figures 5 - 8 show the shearforces, sliding speeds, belt deflections and total deflections (i.e. belt plus tread deflections) for tyre forward speed 1 m/s, tread stiffnesses $c_{px} = c_{py} = 9.0\times10^6$ [N/m^2] and slipvalues κ = 0.02 and α = 0.04 rad. Observe that the maximum beltdeflection and the maximum tread deflection have roughly the same magnitude, which is a consequence of our choice of the stiffnessvalues for treads and belt. Treads and belt contribute in the same order to the total local tyredeflection within the contactarea.

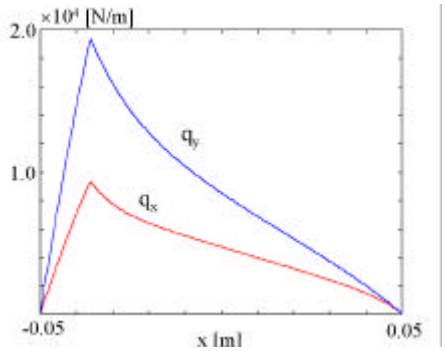

Fig. 5.: Shearforces for (k,a) = (0.02, 0.04) & $c_{px} = c_{py} = 9.0 \cdot 10^6$ [N/m^2]

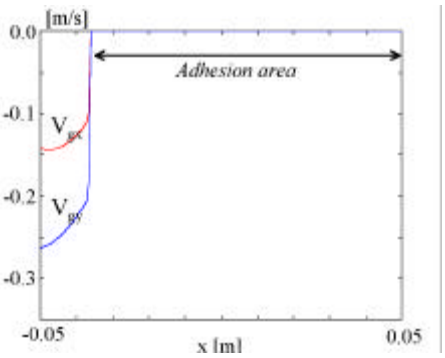

Fig. 6.: Sliding speeds for (k,a) = (0.02, 0.04) & $c_{px} = c_{py} = 9.0 \cdot 10^6$ [N/m^2]

There is only one sliding area. The sliding speeds are discontinous at $x = a_2$, in contrast to the beltdeflections which show a smooth behaviour. The treaddeflections

show a sharp peak at the transition from sliding to adhesion.

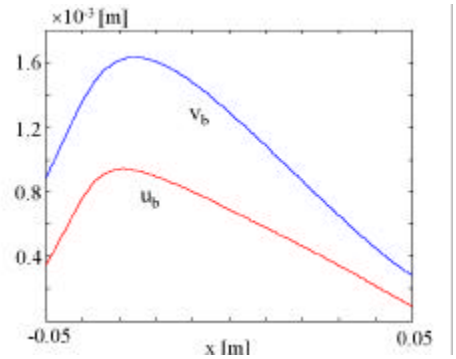

Fig. 7.: Belt deflections for (k,a) = (0.02, 0.04) & $c_{px} = c_{py} = 9.0 \cdot 10^6$ [N/m^2]

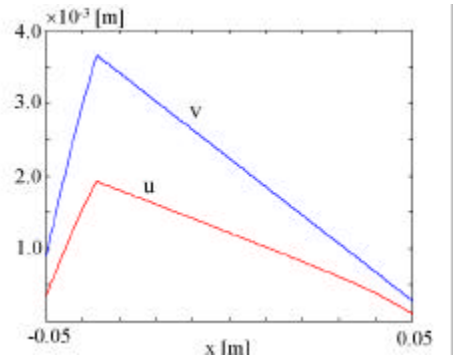

Fig. 8.: Belt deflections for (k,a) = (0.02, 0.04) & $c_{px} = c_{py} = 9.0 \cdot 10^6$ [N/m^2]

The tyre performance can be examined for varying treadstiffness. A 'brush-type' behaviour would be expected for low treadstiffness whereas a 'bare belt-type' behaviour is expected at high treadstiffness. Results for the same slipvalues as used earlier, with equal treadstiffnesses in x- and y-direction varied as indicated in table 3, are shown in figures 9 – 12, restricting to the lateral properties. In the same table 3, the boundaries of the adhesion region are included.

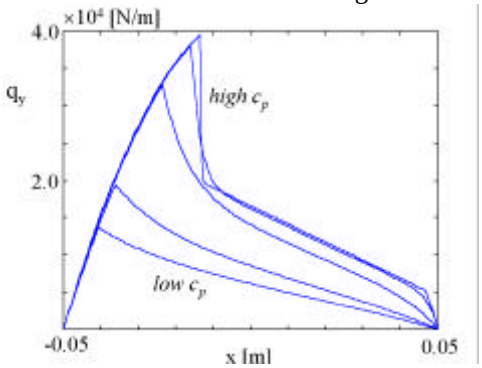

Fig. 9.: Shearforces for (k,a) = (0.02, 0.04) and $c_{px} = c_{py}$ according to table 3

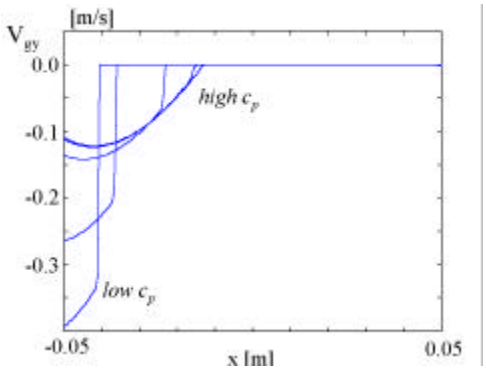

Fig. 10.: Sliding speeds for (k,a) = (0.02, 0.04) and $c_{px} = c_{py}$ according to table 3

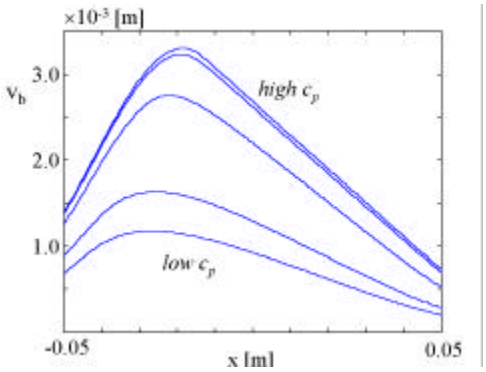

Fig. 11.: .: Belt deflections for (k,a) = (0.02, 0.04) and $c_{px} = c_{py}$ according to table 3

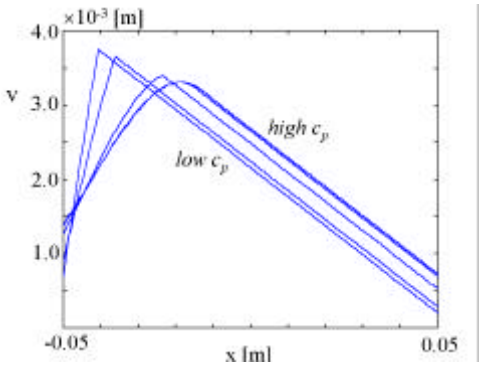

Fig. 12.: Total deflections for (k,a) = (0.02, 0.04) and $c_{px} = c_{py}$ according to table 3

$c_{px} = c_{py}$ [N/m^2]	a_2 [m]	a_1 [m]
5×10^6	-0.0406	0.05
9×10^6	-0.0361	0.05
5×10^7	- 0.0235	0.05
5×10^8	- 0.0158	0.0492
5×10^{10}	- 0.0134	0.0471

Table 3.: Varying treadstiffness

The following conclusions can be drawn with the treadstiffness reduced from very stiff (i.e. with a tyre behaving as a stretched string) to very soft (i.e. with a tyre behaving like a rigid wheel with brushes). The slipvalues and tyreload are not changed. The total deflection appears to remain more or less unchanged whereas the beltdeflection is strongly reduced (and

hence the tread deflection strongly increased). The shape of the total deflection over the contact area changes from rather smooth (dominated by beltdeflection) to a shape with a sharp transition between adhesion and rearward sliding region. For high treadstiffness, two sliding regions are found (see table 3) with the one at the front side of the contact area being very small (in our example about 3 % of the total contact area). With increasing treadstiffness, the transition of the sliding speeds between sliding and adhesion regions becomes less severe, which is explained by the fact that, for the bare string model, the sliding speeds only depend on the belt deflection with continuous slope at $x = a_2$. The adhesion area is enlarged with softer treads, at the cost of higher sliding speeds in the rear sliding region. In other words, softer treads increase the cornering and braking potential of the tyre (e.g. wintertyres versus all-season tyres).

6. CONCLUSIONS

The theoretical combined brush-string tyre model has been treated, including both belt compliance and tread stiffness. The combined slip steady state problem has been solved for this model. The solution has been found using the so-called singular integral approach. This means that the beltequations were replaced by a set of integral equations in terms of contactproperties. The resulting set of nonlinear equations were successfully solved by iteration. Since the singular integral approach is not restricted to the simplified tyre model at hand, it offers new opportunities to generalise the analysis in this paper to more extensive and detailed tyre models, with the complex 3D structure reduced to equations in terms of contact phenomena only, and with more realistic results.

The contactphenomena based on the brush-string tyre model as derived in this paper gives an understanding of local shearforces, deflections of belt and treads as well as the local sliding speeds in lateral and longitudinal directions in relationship with modelparameters such as belt- and treadstiffness. The brush-string model is the continuous transition between the brush-model (i.e. with infinite belt stiffness) and the stretched string model (i.e. with infinite tread stiffness). It has been shown that situations may occur with one or two separate sliding regions, depending on the ratio of belt- and tread stiffness. A dominating beltstiffness leads to a front sliding region, disappearing with reduced tread stiffness. Reducing the treadstiffness also extends the adhesion part in the contactarea at the cost of higher sliding velocities in the sliding part, improving potentially the cornering and braking potential of the tyre.

REFERENCES

[1] Higuchi, A.: *Transient Response of Tyres at Large Wheel Slip and Camber.* Doctoral thesis, Delft University of Technology, Delft, The Netherlands (1997)

[2] Pacejka, H.B.: *The wheel shimmy phenomenon*, Doctoral thesis, Delft University of Technology, Delft, The Netherlands (1966)

[3] Pacejka, H.B.: *The role of tyre dynamic properties*, in.: Pauwelussen, J.P., Pacejka, H.B.: Smart Vehicles, Swets and Zeitlinger Publishers, Lisse (1995)

[4] Pauwelussen, J.P.: *The local contact between tyre and road under steady state slip conditions.* Submitted to Vehicle System Dynamics

[5] Savkoor, A.R.: *The lateral flexibility of pneumatic tires and its application to the lateral rolling contact problem*, SAE paper 700378, FISITA/SAE congress (1970)

[6] Segel, L.: *Force and moment response of pneumatic tyres to lateral motion inputs*, Trans. ASME. J. Engr. for Ind. 88B (1) (1966)

[7] Schlippe, B.v.,Dietrich, R.: *Das Flattern eines bepneuten Rades*, Ber. Lilienthal Ges. 140, p.35 (1941)